metals

MDPI

Article

Cold Roll Bonding of Tin-Coated Steel Sheets with Subsequent Heat Treatment

Illia Hordych, Khemais Barienti *, Sebastian Herbst, Hans Jürgen Maier and Florian Nürnberger

Institut für Werkstoffkunde (Materials Science), Leibniz University Hannover, An der Universität 2, 30823 Garbsen, Germany; hordych@iw.uni-hannover.de (I.H.); herbst@iw.uni-hannover.de (S.H.); maier@iw.uni-hannover.de (H.J.M.); nuernberger@iw.uni-hannover.de (F.N.)

* Correspondence: barienti@iw.uni-hannover.de; Tel.: +49-511-762-9838

Abstract: One possibility to increase the interface strength of cold roll bonded materials is the application of a thin intermediate layer. In the present study, a tin coating was employed to strengthen the interface formed between cold roll bonded steel sheets, and the impact of subsequent heat treatment on the resulting bonding strength was investigated. To increase the bond strength by diffusion, the tin-coated steel bonds underwent heat post-treatment between temperatures of 150 °C and 300 °C for different dwell times. The results demonstrate that the use of tin as an active intermediate layer increases the bond area established. Moreover, the thin tin coating results in the formation of an active intermediate layer that directly takes part in the joining process by establishing a reactive link between the two substrates. A subsequent heat treatment further affects the bond strength by diffusion of tin at the interface.

Keywords: cold roll bonding; cladding; reduction ratio; intermediate layer; tin

Citation: Hordych, I.; Barienti, K.; Herbst, S.; Maier, H.J.; Nürnberger, F. Cold Roll Bonding of Tin-Coated Steel Sheets with Subsequent Heat Treatment. *Metals* **2021**, *11*, 917. https://doi.org/10.3390/met11060917

Academic Editor: Nikki Stanford

Received: 11 May 2021
Accepted: 2 June 2021
Published: 4 June 2021

1. Introduction

Cold roll bonding (CRB) is a rolling operation to join two or more metal sheets at room temperature [1]. CRB has become an economic process for manufacturing components with tailored properties. Compared to hot roll bonding, reduced costs, scale-free surfaces, and the cladding of thin materials such as foils on top of a thicker substrate can be achieved. CRB was shown to be an effective process for bonding similar as well as dissimilar metals depending on the specific demands set by different applications. There is plenty of literature on CRB of steels with other metals such as aluminum [2], copper [3], and titanium [4]. Pan et al. demonstrated the advantages of the cross-shear rolling technique in comparison with conventional rolling, resulting in lowered load forces to obtain the same level of the bond strength [2]. Acoff in cooperation with Chaudhari [5] and Luo [6,7] tested the joining of dissimilar metals such as titanium and aluminum arranged in multilayers. With a developed numerical model using a slab method, they could achieve a good agreement between the numerical and experimental results for the prediction of the bond strength. Nambu et al. investigated the possibilities of joining similar hard martensitic steels with soft austenitic steels by cold rolling [8]. It could be shown that due to such joining the tensile ductility and strength of the bonds could be increased. However, the CRB of steel for employment in structural components remains challenging. To mitigate the required high degree of deformation for creating a bond, intermediate layers placed between the sheets to be bonded were shown to facilitate the formation of firm bonds. Various materials can be employed to support the bond formation of different materials. Kawase et al. used an aluminum hot-dip coating of steel sheets to join them with aluminum sheets [9]. Shabani et al demonstrated an interesting dependence of the bond strength of Cu-Al strips on the thickness of nickel coating. Generally, the coating deteriorated the bond strength; however, applying a thicker nickel coating (>20 µm) resulted in a significant increase of the bonding strength [10]. Organic films have recently also gained importance [11,12] and

have shown promising results. However, a detailed understanding of how the different factors contribute to bond formation is still lacking.

Based on their function, intermediate layers can be divided into active or passive layers [13]. If a bond is effective through an intermediate layer (substrate 1-intermediate layer-substrate 2) and participates directly in the bonding by building a link between the substrates, the intermediate layer is categorized as an active one. To facilitate the function of an active intermediate layer, the material employed should be ductile to be easily spread between the two substrates. In contrast, passive intermediate layers do not directly participate in establishing a bond between the substrates. Before CRB, their function is to prevent oxidation on the surfaces of the substrates that are to be joined. During rolling, these preferably brittle layers are supposed to easily fracture, allowing direct contact of juvenile surfaces of the substrates [14]. Without the addition of intermediate layers, this is conventionally achieved by cleaning [15] and brushing the surface to create a local work-hardening effect and favorable conditions for diffusion joints [16,17]. In particular, the mechanical brushing of surfaces along with the rolling directions before cladding can improve the achieved bonding strength by approximately 4 times compared with unpolished samples, as was shown by Han et al. [18].

In addition, heat treatments are widely used to enhance the materials' properties upon CRB [19]. Depending on the desired effect, the heat treatment can be applied before the CRB process to prepare the bonding partners or after the CRB to improve already formed bonds. In addition, the function of an intermediate layer can be influenced by heat pre-treatment. In previous studies, the application of zinc as well as galfan coatings as passive intermediate layers was investigated [20,21]. Zinc, being more ductile than iron, belongs to the category of the active intermediate layer, yet a successful bonding could not be achieved in these studies. However, intermetallic phases of iron and zinc, which are normally undesired due to their brittleness, can be formed by heat treatments before the CRB process [22]. This resulted in a brittle Zn–Fe-coating that acted as a passive layer and assisted in successfully achieving firm bonds [20]. The additional presence of 5 wt% Al in a galfan coating allowed a cold bonding without the need for an additional heat pre-treatment. Still, a heat pre-treatment further increased the bond strength of the galfan-coated samples [21].

Investigations on the application of heat treatments after the CRB process showed positive results for some specific material combinations, parameters, and conditions [15]. In 1963, Tylecote noticed a positive influence of heat post-treatments for the bonds while investigating the cold joining of copper, aluminum, and steel [23]. For instance, heat treatments of different cladded sheets of copper, aluminum, and steel were reported to increase the bond strength after a short heating period at relatively low temperatures. It was stated that it is essential to prevent the recovery and recrystallization of the metals. Furthermore, it was suggested that thermally activated short-range atomic movements were responsible for the improvement of the bond properties since samples bonded at relatively small deformation showed a larger enhancement of the bond strength. It was assumed that a heat treatment would extend partially bonded interface areas and further increase the bonding strength [23,24]. The formation of brittle intermetallic phases during the heat post-treatments is undesired in contrast to the above-mentioned pre-treatments [3].

To form an active intermediate layer, tin coatings were employed to support the CRB of steel sheets [25]. The effect on the bond strength upon additional heat treatments at 200 °C and 250 °C for dwell times from 15 min up to 90 min after the CRB process were investigated. Diffusion strengthening and the formation of intermetallic phases were suggested to be competing factors for the creation of improved bonding properties.

To further increase the understanding of a strength-relevant effect while employing tin as an active intermediate layer for CRB of steel, the interplay of bond strength, heat post-treatment, and the formation of intermetallics is of current interest. Hence, the influence of different rolling and heat post-treatment conditions was investigated in the present study. Regarding the resulting bonding strength as well as the microscopic bonding quality, the

potential usage of tin as an active intermediate layer was evaluated by mechanical shear tests as well as by light and electron microscopy.

2. Materials and Methods

A low carbon steel DC04 (1.0338) was employed with the following chemical composition determined by glow discharge optical emission spectroscopy (GDOES): C—0.037, Mn—0.251, Si—0.012, P—0.01, S—0.003, Fe—balance (in wt.%). This steel is typically used for flat products produced by cold forming according to DIN EN 10130 [26]. It was chosen due to the low content of alloying elements, which eases to focus on the Fe–Sn interactions. The thickness of the industrially applied (electrochemical deposition) Sn layer employed was 7 to 10 µm.

Before the heat treatment, the tinned steel specimens were symmetrically roll bonded at room temperature with a rolling speed of 0.02 ms^{-1} on a duo rolling mill (Buehler 135—roller diameter 130 mm) following a gradual reduction procedure that was established by the authors in a previous investigation [21]. One pass with reduction ratios (ε) ranging from 43% to 85% was used in the experiments. The sheets were cleaned with acetone in an ultrasonic bath for 5 min to degrease the surface and remove contaminations before the CRB. Next, pairs of specimens with dimensions of 100 mm × 10 mm × 1 mm were positioned with an appropriate overlap to obtain a final bonded length of 25 mm (see Figure 3e). After the bonding process, the specimens were heat post-treated at 150 °C and 300 °C. The former equals a homologous temperature of 0.84 for Sn, and the latter substantially exceeds the melting point of Sn, which equals 232 °C. For the heat treatments, dwell periods of 15 min, 30 min, 60 min, and 90 min were selected. Finally, the samples were air-cooled.

The specimens were embedded, ground, and polished down to a 1µm diamond paste finish to analyze metallographic cross-sections. The prepared samples were investigated by optical microscopy using a DM400M (Leica, Wetzlar, Germany) reflecting-light microscope as well as by scanning electron microscopy (SEM) using a TechSolutions Supra 55VP (Zeiss, Oberkochen, Germany) field emission scanning electron microscope (FE-SEM).

Laser microscopy was applied to evaluate the bond continuity along the cross-section. Per specimen, 30 images were taken with a VK-97103D Laser Scanning Confocal Microscope (Keyence, Neu-Isenburg, Germany), were analyzed, and provided topographical height measurements. Figure 1 shows an example of an image with three superimposed lines indicating typical traces used for the height measurements. While the blue line passes through a well-bonded region, the red and green lines correspond to regions that were not bonded. In the following, the two different types of interfaces are referred to as: bonded region b (see Figure 1b blue line) and defects d featuring oxidized spots, pores, etc. (see Figure 1b red and green lines). The total representative length of each section was determined via a threshold method and is presented as a fraction of the entire length (5 mm) of the analyzed interfaces.

The mechanical properties of the bonds were measured in a tensile shear test using a Z010 tensile machine (Zwick Roell, Ulm, Germany) with a maximum load capacity of 10 kN at a constant crosshead speed of 1 mm min^{-1}. The samples were strained until delamination occurred. Since the sample fracture behavior was brittle, values of the elongation at failure were not determined.

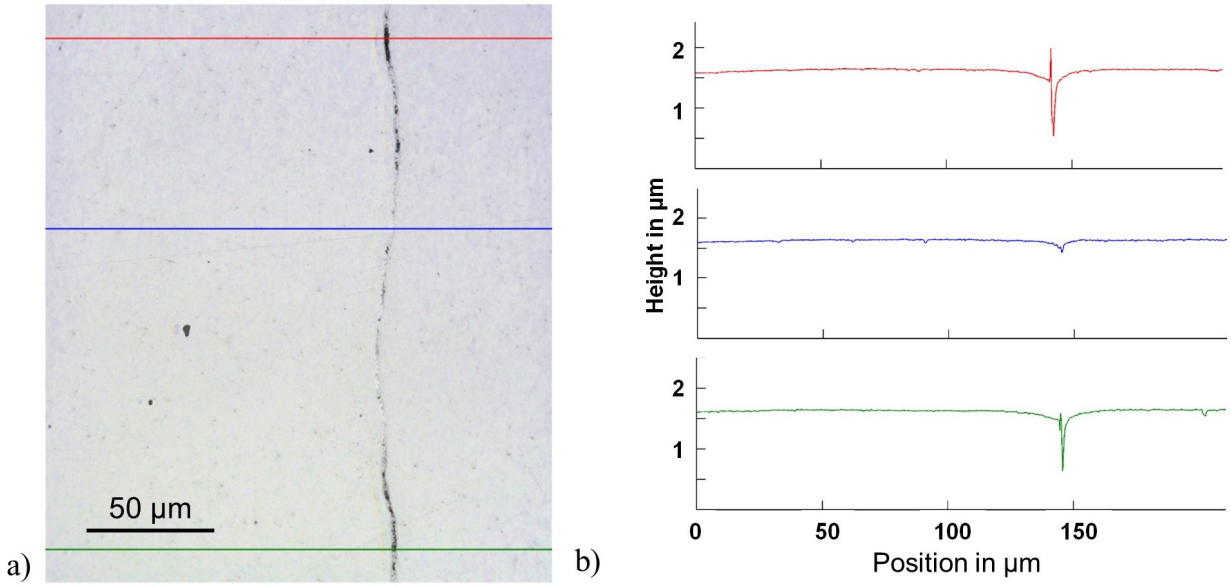

Figure 1. Optical analysis of the bond continuity (**a**) and selective height measurements (**b**).

3. Results and Discussion

Results of the shear-tensile test for the non-heat-treated samples as a function of the reduction ratio are shown in Figure 2a. The absolute values of the bond strength appear rather low. However, considering the tensile strength of pure tin of 14.5 MPa at room temperature [27], up to 60% of the strength of tin was achieved. The bond strength of the non-heat-treated samples demonstrates a clear dependence on the reduction ratio. From Figure 2a, the threshold strain for creating a bond is roughly 55%. However, a firm bond was achieved when exceeding a total strain of about 65%. The transition occurs between 60% and 65%. Above these reduction values, similar values with some discrepancies in the bond strength can be noticed. It assumes the essential influence of the threshold deformation: Once the bond is created by overcoming 65% of reduction, some level of the strength can be achieved without its clear enhancement due to further increase of the reduction.

Figure 2b,c depict representative micrographs of the samples' interfaces that were bonded with a total deformation of 56.5% and 79%. The first example (56.5%, Figure 2b) features a visible gap of around 2 µm between both sides, while the bonded area of the second one (79%, Figure 2c) can hardly be recognized anymore due to the significant thinning of the Sn intermediate layer by more than 90%. Despite the large deformation, no discontinuities of the Sn layer were observed.

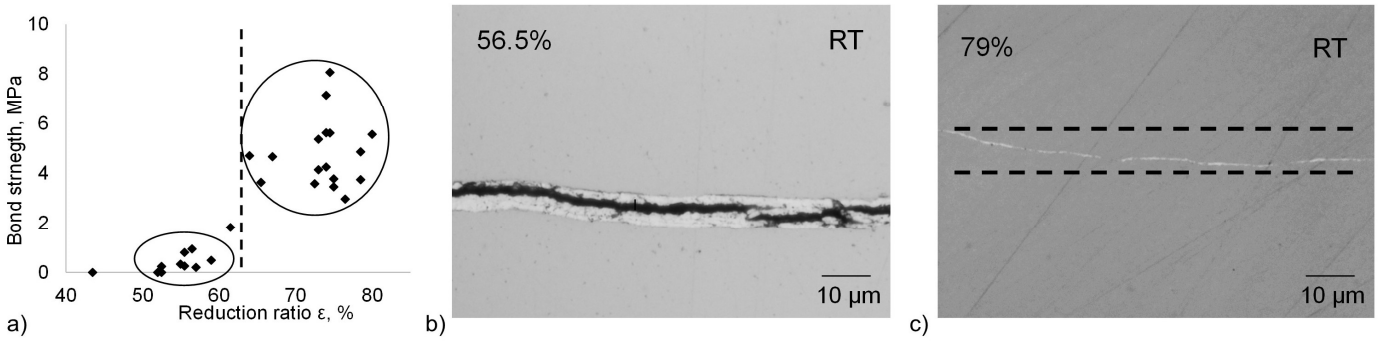

Figure 2. Bond strength of the samples bonded without heat treatment as a function of the reduction (**a**); interfaces of selected samples rolled with reduction ratios of 56.5% (**b**) and 79% (**c**).

For the heat-treated samples, the dependence of the mechanical properties on the reduction ratio during CRB is much less pronounced. Instead, the established bond strength becomes less reliant on the rolling parameters and is mainly influenced by the heat-treatment parameters. The analysis of the resulting bond strength as a function of dwell time for each treating temperature reveals the dominant influence of the heat treatments and the temperature–time course (Figure 3). The bond strength increases linearly up to a dwell time of 90 min for heat treatment at 150 °C (coefficient of determination R^2 = 0.92; p-value = 0.043); due to this dependence, the prolongation of the dwell time beyond 90 min might be of further interest for this temperature in future experiments. Increasing the temperature to 200 °C represents a transitional zone with no clear reliance on the dwell time (R^2 = 0.03; p-value = 0.769). A further increase in temperature to 250 °C inverses the positive trend and results in the linear decrease of the bond strength with longer dwell time (R^2 = 0.77; p-value = 0.05). At 300 °C, the bond strength is independent of the dwell time and the reduction ratio (R^2 = 0.23; p-value = 0.337). Comparing all investigated heat treatment conditions, it becomes evident that short heat post-treatments at moderate temperatures lead to the highest bond strength.

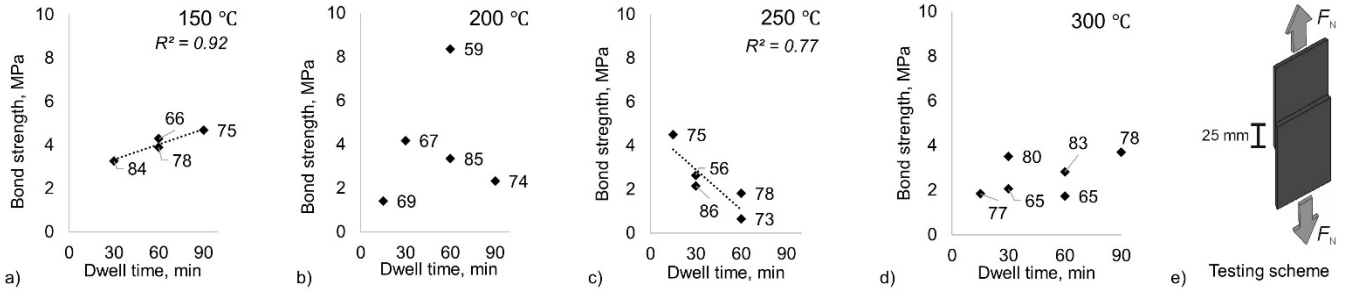

Figure 3. Bond strength as a function of dwell time at 150 °C (**a**), 200 °C (**b**) [23], 250 °C (**c**) [23], and 300 °C (**d**), with the corresponding reduction ratios of the specimens given in % as is represented as the datapoint label and the employed testing scheme (**e**).

To further explore this behavior, SEM investigations were performed. These as well as the results from [25] were supported with EDX line scans of the interfaces to further examine the effects of the heat treatment on the bonding properties. Figure 4a,b depict the bond zones of the samples without a heat treatment and those treated for 30 min at 200 °C. The Sn content in the non-treated sample interface appears to reach a mass fraction of up to 90%, although the true value is assumed to be 100%. This difference is due to the lateral resolution of the EDX measurement being in the same range as the interlayer width. Still, a meaningful relative comparison of the samples can be conducted. In Figure 4b, a wider interface with an increased Fe mass fraction can be seen, which implies a bidirectional diffusion of tin and iron. In the interface, small fractions of intermetallics can be observed. For the 250 °C/30 min case (Figure 4c), an uneven interface with a sharp transition from steel to tin can be observed. This indicates a changing nature of the interface and points to the formation of intermetallics. A comparison of Figure 4c,d highlights the influence of the dwell time at an identical treatment temperature. In this case, the interfacial layer propagated into the steel matrix, and the average thickness of the interfacial layer enlarged by a factor of 3. The analysis of the composition shows the formation of an intermetallic phase with a constant proportion of the elements over a greater measuring length in Figure 4d [28]. The composition matches that of the intermetallic phase $FeSn_2$.

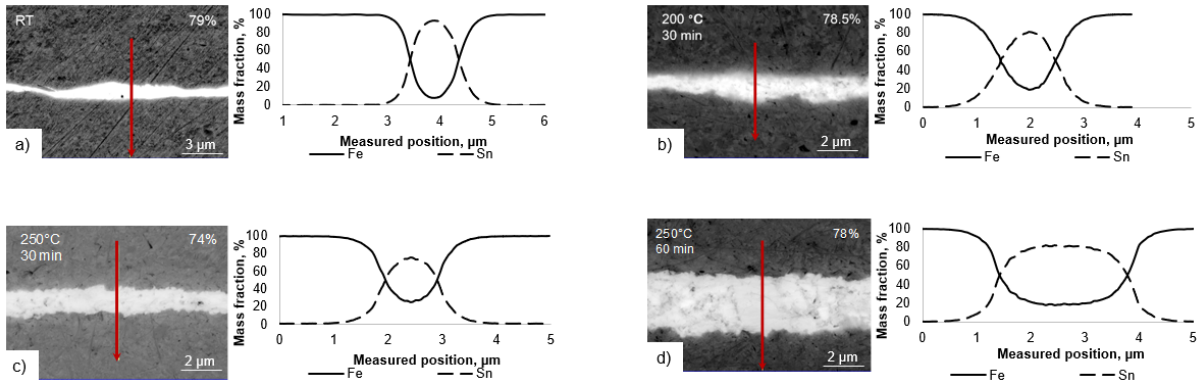

Figure 4. SEM images and corresponding line scans, along with the bonded interface in the initial state (**a**) as well as after the heat treatments at 200 °C for 30 min (**b**), at 250 °C for 30 min (**c**), and 60 min (**d**).

To increase the lateral resolution of the EDX measurement and to analyze the transition zone concerning the formation of intermetallic phases, a FIB lamella with dimensions of 16 µm × 9 µm × 70 nm was prepared from the interfacial zone of the sample shown in Figure 4c, cf. Figure 5.

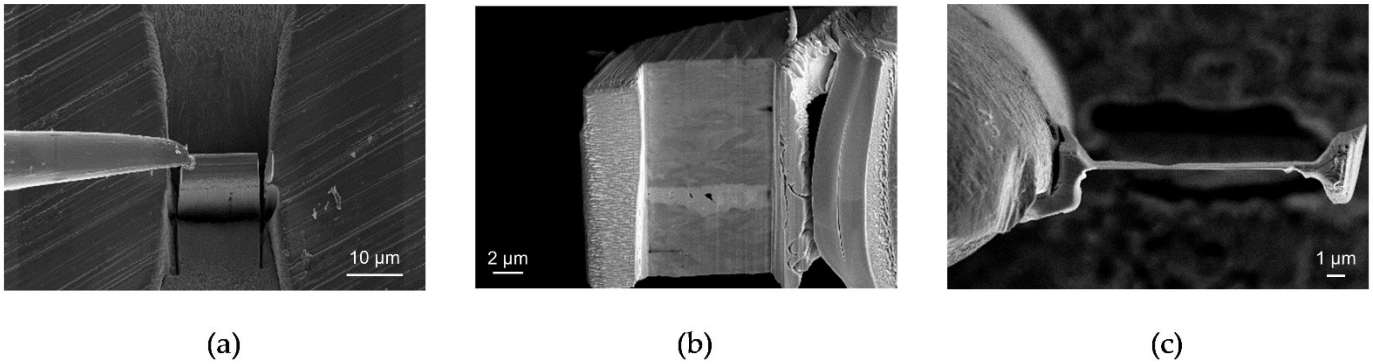

Figure 5. Preparation of a FIB lamella from the sample treated at 250 °C for 30 min: (**a**) coarse cut, (**b**) front view, (**c**) top view.

The EDX analysis of the lamella revealed the distribution of Fe and Sn in the transition zone as depicted in Figure 6. Two line scans perpendicular to the interfacial layer displaying the proportion of Sn and Fe in wt.% are shown in Figure 6b,c. The sharp transition between both elements implies that the previous solid solution of Sn and Fe transformed into an intermetallic phase with a fixed stoichiometry. The measured composition of the interfacial layer along line 1 consists of 64.4 ± 1.1% of Sn and 35.4 ± 1.2% of Fe. Line 2 confirms these values with 63.6 ± 2.8% of Sn and 36.3 ± 2.8% of Fe. This composition implies the formation of the intermetallic phase $FeSn_2$ [28]. These measurements support the previous assumption of the formation of intermetallic phases at 250 °C after a dwell time of only 30 min.

Due to the small area probed, an evaluation using SEM alone cannot give a comprehensive overview of the condition of the interface. Hence, a more macroscopic evaluation was performed using laser microscopy for selected specimens, with the best interfaces as determined by SEM. The fraction of the bonded interface for each investigated condition is shown in Figure 7. It can be stated that the application of heat treatment in general as well as the increase of temperature and dwell time leads to an increase of the defect fraction (pores and oxidized spots) and thus to the deterioration of the bonded interface. Due to direct contact of the specimens with the atmosphere and partial diffusion of oxygen atoms along the interfaces towards the center areas, the quality of the bond tends to be negatively affected.

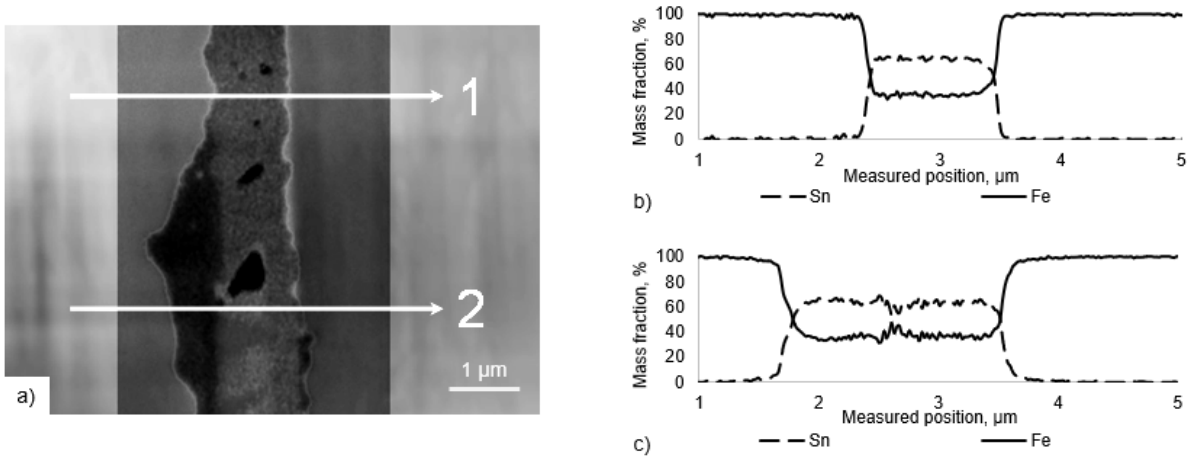

Figure 6. Image of the FIBed section from the sample treated at 250 °C for 30 min (**a**) and corresponding line scans (**b**,**c**).

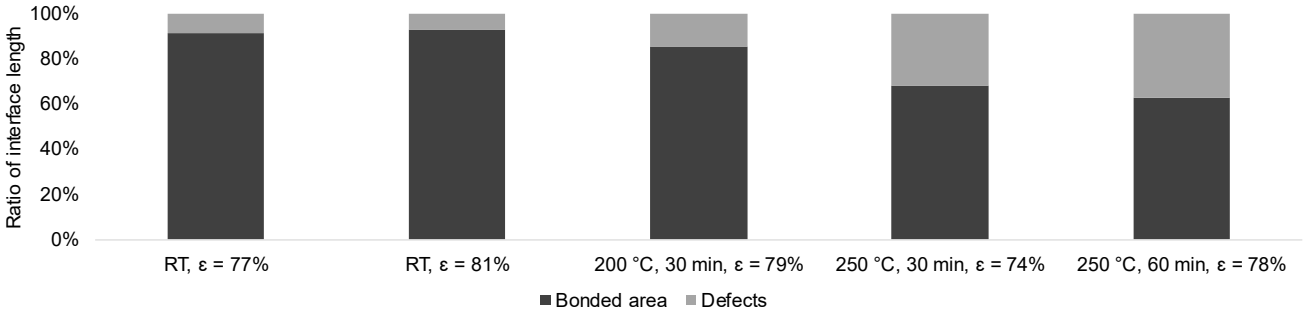

Figure 7. Bond area continuity analysis for different heat treatment parameters and reduction ratios.

Taking the SEM results and mechanical properties into account, it can be concluded that different processes are responsible for the change of the bond properties due to the heat treatment. As the treatment temperature and duration increase, the diffusivity of tin, iron, and oxygen atoms does as well. Up to 200 °C, this leads to an improvement of the bond properties by mutual diffusion of Fe and Sn atoms. Thus, the strengthening of the Fe–Sn bonds dominates over the negative effects of oxidation. The presented results are in accord with those presented in Reference [23], where an improvement of the bond strength was observed at low temperatures, but a decrease was observed with higher temperatures. The results of the present study also indicate that subsequent heating after the CRB process provokes surface diffusion along small interface defects. Sn atoms can be assumed to migrate from the Sn layers that are not bonded to already bonded parts of the interface. Once the Sn atoms reach these micro-bonded regions, they contribute to the strengthening of the existing bond. Given this scenario, the strength of weakly bonded areas is improved by diffusion during the heat treatment, increasing the macro strength [23]. At 200 °C, the active formation of the intermetallic phase $FeSn_2$ as well as the increased oxidation lead to a deterioration of the bond quality.

Abbasi [24] determined a critical thickness for the intermetallic layer of 2.5 µm for Al/Cu bimetals for which the behavior of the intermetallics changes from ductile to brittle, resulting in a decrease in bond strength. Similarly, the present investigations have demonstrated that intermetallic tracks of up to 1 µm do not negatively affect the bond strength and that bond strength decreases with a layer width beyond this value.

The employment of tin as an active intermediate layer results in a good bonding quality, which regarding its bond strength is nonetheless limited by the properties of the tin coating itself. Further improvement of the CRB of steel could be achieved by substituting tin with another element such as nickel. In addition to the usage of an intermediate layer, other possible improvements of the CRB process are in the focus of the community. A

promising method for further decreasing the needed reduction ratio was shown effective for Cu/Al composite by Wang et al. [29,30]. They propose a novel corrugated + flat rolling (CFR) method, which uses a two-step process to achieve a stable bonding interface. In this approach, the composite is first rolled with a corrugated roll and afterwards flattened using a conventional roller. In addition, a novel way of controlling processing conditions in terms of the ambient atmosphere could lead to radical improvements in the CRB process in general. To completely circumvent the negative effect of oxidation during processing, the employment of extreme high vacuum (XHV)-adequate conditions was demonstrated to be highly effective [25,31]. Specifically, the application of a SiH_4-doped inert gas atmosphere can limit the ambient oxygen concentration to about 10^{-23} ppm and thus can fully prevent oxidation during processing. Employing an XHV-adequate atmosphere during the whole CRB process might allow the bond properties to further increase, and detailed work is underway to address this issue.

4. Conclusions

The effect of heat post-treatment on the bond strength upon cold roll bonding was studied for tin-coated steel sheets. The main results and conclusions follow.

The mechanical bonding strength of specimens without subsequent heat treatments exhibits a positive correlation with the reduction ratio above a threshold value of about 65%. However, this correlation becomes negligible after heat treatment.

Bond strength can be increased by heat post-treatment due to the mutual diffusion of iron and tin; already micro-bonded areas are strengthened further. The strengthening effect weakens if the bond was already well established beforehand. Due to the heat post-treatments at intermediate temperatures for tin (up to 200 °C) and lower dwell durations up to 90 min, these bonds elevated their strength to the level of the bonding conditions with higher reduction ratios and without subsequent heat treatments. The resulting bonding strength remains limited by tin's yield strength.

At elevated temperature (≈200 °C), the formation of intermetallic phases and interface oxidation induced by the increased diffusion of tin, oxygen, and iron atoms starts to negatively affect the bond quality.

A threshold for the thickness of the intermetallic of about 1 µm was determined. Thus, a larger intermetallic should be avoided, as it could result at reductions below the threshold combined with prolonged heat treatments above 200 °C.

Given the negative effect of oxidation and the formation of the intermetallic layer, lower temperatures of the heat post-treatment and shorter dwell times are thus more beneficial for the improvement of the bond properties.

Author Contributions: Conceptualization, S.H., F.N., I.H, and H.J.M.; investigation, I.H.; writing—original draft preparation, I.H. and K.B.; writing—review and editing, K.B., S.H., F.N., and H.J.M.; visualization, I.H. and K.B.; supervision, F.N. and H.J.M. All authors have read and agreed to the published version of the manuscript.

Funding: This research was funded by the Deutsche Forschungsgemeinschaft (DFG, German Research Foundation)—Project-ID 394563137—SFB 1368.

Institutional Review Board Statement: Not applicable.

Informed Consent Statement: Not applicable.

Data Availability Statement: Not applicable.

Acknowledgments: For the assistance with the rolling experiments, special thanks go to Michael Rodman, Mehmet Fazil Kapci, and Burak Bal.

Conflicts of Interest: The authors declare no conflict of interest.

References

1. Wright, P.K.; Snow, D.A.; Tay, C.K. Interfacial conditions and bond strength in cold pressure welding by rolling. *Met. Technol.* **1978**, *5*, 24–31. [CrossRef]
2. Pan, D.; Gao, K.; Yu, J. Cold roll bonding of bimetallic sheets and strips. *Mater. Sci. Technol.* **1989**, *5*, 934–939. [CrossRef]
3. Manesh, H.D.; Taheri, A.K. Bond strength and formability of an aluminum-clad steel sheet. *J. Alloys Compd.* **2003**, *361*, 138–143. [CrossRef]
4. Dziallach, S.; Bleck, W.; Köhler, M.; Nicolini, G.; Richter, S. Roll-Bonded Titanium/Stainless-Steel Couples, Part 1: Diffusion and Interface-Layer Investigations. *Adv. Eng. Mater.* **2009**, *11*, 75–81. [CrossRef]
5. Chaudhari, G.P.; Acoff, V. Cold roll bonding of multi-layered bi-metal laminate composites. *Compos. Sci. Technol.* **2009**, *69*, 1667–1675. [CrossRef]
6. Luo, J.G.; Acoff, V. Using cold roll bonding and annealing to process Ti/Al multi-layered composites from elemental foils. *J. Mater. Sci. Eng. A* **2004**, *379*, 164–172. [CrossRef]
7. Luo, J.G.; Acoff, V.L. Processing gamma-based TiAl sheet materials by cyclic cold roll bonding and annealing of elemental titanium and aluminum foils. *J. Mater. Sci. Eng. A* **2006**, *433*, 334–342. [CrossRef]
8. Nambu, S.; Michiuchi, M.; Inoue, J.; Koseki, T. Effect of interfacial bonding strength on tensile ductility of multilayered steel composites. *Compos. Sci. Technol.* **2009**, *69*, 1936–1941. [CrossRef]
9. Kawase, B.H.; Makimoto, M.; Takagi, K.; Ishida, Y.; Tanaka, T. Development of Aluminum-clad Steel Sheet by Roll-bonding. *Trans. Iron Steel Inst. Jpn.* **1983**, *23*, 628–632. [CrossRef]
10. Shabani, A.; Toroghinejad, M.R.; Shafyei, A. Effect of post-rolling annealing treatment and thickness of nickel coating on the bond strength of Al–Cu strips in cold roll bonding process. *Mater. Des.* **2012**, *40*, 212–220. [CrossRef]
11. Hoppe, C.; Ebbert, C.; Voigt, M.; Schmidt, H.C.; Rodman, D.; Homberg, W.; Maier, H.J.; Grundmeier, G. Molecular Engineering of Aluminum–Copper Interfaces for Joining by Plastic Deformation. *Adv. Eng. Mater.* **2016**, *18*, 1066–1074. [CrossRef]
12. Schmidt, H.C.; Homberg, W.; Orive, A.G.; Grundmeier, G.; Hordych, I.; Maier, H.J. Cold pressure welding of aluminum-steel blanks: Manufacturing process and electrochemical surface preparation. *AIP Conf. Proc.* **2018**, *1960*, 50007. [CrossRef]
13. Bay, N.; Zhang, W.; Jensen, S.S. The application of strategic surface coatings to improve bonding in solid phase welding. *Int. J. Join. Mater.* **1994**, *6*, 47–57.
14. Bay, N.; Clemensen, C.; Juelstorp, O.; Wanheim, T. Bond Strength in Cold Roll Bonding. *CIRP Ann.* **1985**, *34*, 221–224. [CrossRef]
15. Li, L.; Nagai, K.; Yin, F. Progress in cold roll bonding of metals. *Sci. Technol. Adv. Mater.* **2008**, *9*, 1–11. [CrossRef]
16. Wang, C.; Jiang, Y.; Xie, J.; Zhou, D.; Zhang, X. Effect of the steel sheet surface hardening state on interfacial bonding strength of embedded aluminum–steel composite sheet produced by cold roll bonding process. *J. Mater. Sci. Eng. A* **2016**, *652*, 51–58. [CrossRef]
17. Qiu, Y.; Kaden, N.; Schmidtchen, M.; Prahl, U.; Biermann, H.; Weidner, A. Laminated TRIP/TWIP Steel Composites Produced by Roll Bonding. *Metals* **2019**, *9*, 195. [CrossRef]
18. Han, J.; Niu, H.; Li, S.; Ren, Z.; Jia, Y.; Wang, T.; Plokhikh, A.I.; Huang, Q. Effect of Mechanical Surface Treatment on the Bonding Mechanism and Properties of Cold-Rolled Cu/Al Clad Plate. *Chin. J. Mech. Eng.* **2020**, *33*, 69. [CrossRef]
19. Tsuji, N.; Ito, Y.; Saito, Y.; Minamino, Y. Strength and ductility of ultrafine grained aluminum and iron produced by ARB and annealing. *Scr. Mater.* **2002**, *47*, 893–899. [CrossRef]
20. Hordych, I.; Rodman, D.; Nürnberger, F.; Hoppe, C.; Schmidt, H.C.; Grundmeier, G.; Homberg, W.; Maier, H.J. Effect of Pre-Rolling Heat Treatments on the Bond Strength of Cladded Galvanized Steels in a Cold Roll Bonding Process. *Steel Res. Int.* **2016**, *87*, 1619–1626. [CrossRef]
21. Hordych, I.; Rodman, D.; Nürnberger, F.; Schmidt, H.C.; Orive, A.G.; Homberg, W.; Grundmeier, G.; Maier, H.J. Influence of heat-pretreatments on the microstructural and mechanical properties of galfan-coated metal bonds. *AIP Conf. Proc.* **2018**, *1960*, 40007. [CrossRef]
22. Herbst, S.; Maier, H.J.; Nürnberger, F. Strategies for the Heat Treatment of Steel-Aluminium Hybrid Components. *J. Heat Treat. Mater.* **2018**, *73*, 268–282. [CrossRef]
23. Tylecote, R.F.; Wynne, E.J. Effect of Heat Treatment on Cold Pressure Welds. *Br. Weld. J.* **1963**, 385–394.
24. Abbasi, M.; Taheri, A.K.; Salehi, M.T. Growth rate of intermetallic compounds in Al/Cu bimetal produced by cold roll welding process. *J. Alloys Compd.* **2001**, *319*, 233–241. [CrossRef]
25. Schmidt, H.C.; Orive, A.G.; Hordych, I.; Herbst, S.; Nürnberger, F.; Homberg, W.; Grundmeier, G.; Maier, H.J. Joining of blanks by cold pressure welding: Incremental rolling and strategies for surface activation and heat treatment. *Materialwiss. Werkstofftech.* **2019**, *50*, 924–939. [CrossRef]
26. DIN EN 10130:2007-02. *Kaltgewalzte Flacherzeugnisse Aus Weichen Stählen Zum Kaltumformen—Technische Lieferbedingungen. Deutsche Fassung EN 10130:2006*; Beuth Verlag GmbH: Berlin, Germany, 2007.
27. Graf, G.G. Tin, Tin Alloys, and Tin Compounds. *Ullmann's Encycl. Ind. Chem.* **2012**, *37*, 1–33. [CrossRef]
28. Predel, B.; Madelung, O. *Fe-Sn (Iron-Tin). Dy-Er–Fr-Mo. Landolt-Börnstein-Group IV Physical Chemistry (Numerical Data and Functional Relationships in Science and Technology)*; Springer: Berlin/Heidelberg, Germany, 1995.
29. Wang, T.; Li, S.; Ren, Z.; Han, J.; Huang, Q. A Novel Approach for Preparing Cu/Al Laminated Composite Based on Corrugated Roll. *Mater. Lett.* **2019**, *234*, 79–82. [CrossRef]

30. Wang, T.; Li, S.; Ren, Z.; Jia, Y.; Fu, W.; Guo, M.; Ma, X.; Han, J. Microstructure Characterization and Mechanical Property of Mg/Al Laminated Composite Prepared by the Novel Approach: Corrugated + Flat Rolling (CFR). *Metals* **2019**, *9*, 690. [CrossRef]
31. Holländer, U.; Wulff, D.; Langohr, A.; Möhwald, K.; Maier, H.J. Brazing in SiH_4-Doped Inert Gases: A New Approach to an Environment Friendly Production Process. *Int. J. Precis. Eng. Manuf. Green Tech.* **2019**, *7*, 1059–1071. [CrossRef]